https://doi.org/10.5194/acp-2022-752
Preprint. Discussion started: 14 November 2022

Atmospheric Chemistry and Physics Discussions

Impact of aerosol optics on vertical distribution of ozone

Shuqi Yan[2], Bin Zhu[1,*], Shuangshuang Shi[1], Wen Lu[1], Jinhui Gao[3], Hanqing Kang[1], Duanyang Liu[2]

[1]Collaborative Innovation Center on Forecast and Evaluation of Meteorological Disasters, Key Laboratory for Aerosol-Cloud-Precipitation of China Meteorological Administration, Key Laboratory of Meteorological Disaster, Ministry of Education (KLME), Special Test Field of National Integrated Meteorological Observation, Nanjing University of Information Science & Technology, Nanjing 210044, China
[2]Key Laboratory of Transportation Meteorology of China Meteorological Administration, Nanjing Joint Institute for Atmospheric Sciences, Nanjing 210041, China
[3]Plateau Atmosphere and Environment Key Laboratory of Sichuan Province, School of Atmospheric Sciences, Chengdu University of Information Technology, Chengdu 610225, China

Correspondence to: Bin Zhu (binzhu@nuist.edu.cn)

Abstract. Tropospheric ozone, an important secondary pollutant, is greatly impacted by aerosols within boundary layer (BL). Previous studies have mainly attributed ozone variation to either aerosol-BL or aerosol-photolysis interactions at near surface. In this study, we analyze the sensitivities of ozone response to aerosol mixing states (e.g., mixing behaviour hypothesis of scattering and absorbing components) in the vertical direction and address the effects of aerosol-BL and aerosol-photolysis interactions on ozone profiles by WRF-Chem simulations. The aerosol internal mixing state experiment reasonably reproduces the vertical distribution and time variation of meteorological elements and ozone. Sensitive experiments show that aerosols lead to turbulent suppression, precursor accumulation, lower-level photolysis reduction and upper-level photolysis enhancement. Consequently, ozone basically decreases within entire BL during daytime (08:00~17:00), and the decrease is the least in external mixing state (0.6%) compared with internal (9.8%) and core-shell mixing states (7.4%). The photolysis enhancement is the most significant in external mixing state due to its strong scattering ability. By process analysis, lower-level ozone chemical loss is enhanced due to photolysis reduction and NO_X accumulation under VOC-limited regime. Upper-level ozone chemical production is accelerated due to higher photolysis rate resulting from aerosol backscattering. Therefore, the increased ozone entrainment from aloft BL to surface induced by boosted ozone vertical gradient outweighs the decreased ozone entrainment induced by turbulent suppression after 11:00 am. Additional simulations support that aerosol effect on precursor, photolysis and ozone is consistent under different underlying surface and pollution conditions.

1 Introduction

Tropospheric ozone is an important secondary pollutant that is produced by the photochemistry of VOC (volatile organic compounds) and NO_x. The variation of ozone is determined by the highly variable interactions among meteorology, precur-

https://doi.org/10.5194/acp-2022-752
Preprint. Discussion started: 14 November 2022


Atmospheric Chemistry and Physics Discussions

sors, photochemistry and aerosols. Tropospheric ozone, especially in the atmospheric boundary layer (BL), exerts side effects such as impairing human health, contributing to global warming and aggravating air pollution (Fu et al., 2019). Since 2013, the severe $PM_{2.5}$ pollution over East China has been mitigated but ozone concentration is increasing (Li et al., 2020). Therefore, the characteristic of ozone variation and its relationship with external factors need to be intensively studied.

The interactions between ozone and aerosols are complicated and have attracted wide concern in recent years. Aerosols can significantly affect ozone photochemistry by influencing photolysis process (herein called aerosol-photolysis interaction). The weakened solar radiation reaching the ground induced by aerosol extinction can decrease photolysis rate at the surface and within several hundred meters above the surface, thus inhibiting ozone production and resulting in lower ozone concentration (Gao et al., 2020; Jacobson, 1998; Li et al., 2011). Contrarily, scattering aerosols increase upward shortwave radiation which may promote ozone formation at a higher altitude (Gao et al., 2021a). Dickerson et al. (1997) and Shi et al. (2022) demonstrated that aerosol pollution can remarkably increase ultraviolet radiation at a few hundred meters above the aerosol layer, which accelerates photolysis and increase ozone concentration by about 3~20 ppb. Additionally, heterogeneous reactions on aerosol surface can also influence ozone chemistry (Jacob, 2000; Li et al., 2019; Lou et al., 2014).

Aerosols affect BL thermodynamics and ultimately result in ozone change, which has attracted much attention in recent years. The perturbation in radiation flux profile induced by aerosols can alter BL structure, thus influencing vertical mixing and affecting ozone and precursor concentration (herein called aerosol-BL interaction). Aerosols stabilize BL and suppress turbulent mixing (Ding et al., 2016; Li et al., 2017), which can inhibit the vertical exchange of ozone. Gao et al. (2018) studied the effect of black carbon (BC) on ozone variation within BL. BC weakens turbulent mixing and inhibits the higher ozone aloft being entrained downward. Additionally, the suppression of BL leads to the accumulation of NO_x which promotes the formation of radicals and chemical production of ozone. The weakening in ozone mixing outweighs the enhancement in ozone chemical production, so the surface ozone is decreased during the daytime.

The mixing behaviour hypothesis of aerosol scattering and absorbing components yields three major mixing states: internal mixing, core-shell mixing and external mixing. In internal and core-shell mixing, aerosol light absorption can be enhanced by 50~100% (Bond et al., 2006; Jacobson, 2001). In external mixing, the absorption ability is weaker but scattering ability is stronger (Zeng et al., 2019). Accordingly, aerosol mixing behaviour alters aerosol optical properties and affects its interactions with BL and photolysis. Gao et al. (2021b) found that aerosols result in smaller boundary layer height (PBLH) reduction in external mixing (11.6 m) than in core-shell mixing (24 m), consequently leading to different changes in photolysis rates and ozone concentration.

Many studies reveal the aerosol effect on ozone at near-surface level. Aerosols notably affect ozone photochemistry at all heights within BL and ultimately influence ozone vertical distribution and turbulent exchange. Therefore, the aero-

https://doi.org/10.5194/acp-2022-752
Preprint. Discussion started: 14 November 2022


Atmospheric Chemistry and Physics Discussions

sol-induced ozone variation could have larger complexity and uncertainty in the vertical direction, which should be explored further. Additionally, previous studies explain ozone variation mainly by either aerosol-BL or aerosol-photolysis interaction, but relatively few of them consider these two mechanisms together. In this study, we aim to quantitatively reveal the impact of aerosols on ozone profile through the two pathways (aerosol-BL and aerosol-photolysis interactions) by WRF-Chem simulations, as well as how aerosol effect varies with aerosol mixing states. Heterogeneous chemistry is not included in this study. The manuscript is organized as follows. Section 2 introduces the data, model and sensitive experiments. Section 3.1 evaluates the model performances. Sections 3.2 to 3.4 reveal the characteristic of aerosol-BL and aerosol-photolysis interactions and their impacts on ozone variation. Section 4 performs additional analysis and simulations to support the results. Section 5 concludes the findings of this study.

2 Data, model and experiments

2.1 Data

A field campaign was conducted at an industrial zone in north Nanjing suburban (118.71°E, 32.27°N; Figure 1) in November 2020. We collected the vertical profiles of meteorological elements (temperature, wind speed and direction) and air pollutants ($PM_{2.5}$, BC and ozone). Meteorological elements are observed at 08:00 and 14:00, and air pollutants are observed four times a day at around 09:00, 11:00, 14:00 and 16:00 (local times). The introduction of observation instruments can be referred to Shi et al. (2020). These data are used to evaluate the model performance in the vertical direction. The model performance on meteorology and pollutants is generally reasonable during the whole observation period. We mainly use the data from 2 to 5 November to study the effect of aerosols on ozone, and detailly investigate the physical and chemical mechanisms in the pollution stage on 2 November. The ground observation data includes the MICAPS hourly data (Li et al., 2010) from Pukou site (118.60°E, 32.05°N) which is the nearest weather station close to the observation site. We use the temperature, wind speed and direction to evaluate the model performance on the time series of meteorological elements.

2.2 Model configuration and sensitive experiments

The model used in this study is the WRF-Chem (V3.9.1.1) model. It is the state-of-the-art atmospheric model that online couples meteorology and chemistry. Two domains are set up with the central point at the observation site (118.71°E, 32.27°N) (Figure 1). The parent domain has the size of 79×79 grids with the grid spacing of 27 km. The inner domain has the size of 79×79 grids with the grid spacing of 9 km. To better describe the turbulent process, the vertical level is refined to 38 layers and 12 of which are below 2 km. All the model results are calculated at the nearest grid close to the observation site if not specified.

https://doi.org/10.5194/acp-2022-752
Preprint. Discussion started: 14 November 2022


Atmospheric Chemistry and Physics Discussions

The anthropogenic emission inventory is provided by MEIC from Tsinghua University (Zheng et al., 2018) (http://www.meicmodel.org/). MEIC includes major gaseous and aerosol species, e.g., SO_2, NH_3, VOCs, NO_x, BC, $PM_{2.5}$ and PM_{10}. The gas chemical mechanism is Carbon Bond Mechanism Z (CBMZ; Zaveri and Peters, 1999), and the aerosol chemical mechanism is Model for Simulating Aerosol Interactions and Chemistry with four bins (MOSAIC-4bin; Zaveri et al., 2008). These two chemical mechanisms are widely used for studying ozone chemistry. Detailed physical and chemical schemes are listed in Table 1.

The initial and boundary fields of meteorology are provided by ERA5 0.25°×0.25° reanalysis data (https://cds.climate.copernicus.eu/cdsapp#!/dataset/reanalysis-era5-pressure-levels?tab=form). The chemical initial and boundary fields are provided by WACCM (https://www2.acom.ucar.edu/gcm/waccm). The simulation starts at 08:00 on 30 October and ends at 20:00 on 2 November, and the first 72h is spin-up period. All the time here is local time (UTC+8).

In this work, the effect of aerosol optics on ozone profiles is addressed by its mixing states. We study three types of mixing states: internal mixing, core-shell mixing and external mixing, which depend on the mixing behaviour hypothesis of scattering and absorbing components. Only the external mixing is not included in the current WRF-Chem model. The calculation of aerosol optical properties and how to add the code for external mixing can be referred to Gao et al. (2021b). To study the aerosol effect on ozone, four experiments are conducted (Table 2). The case "int" is the base experiment (the default option in WRF-Chem), in which the aerosols are internally mixed. The cases "csm" and "ext" are core-shell mixing and external mixing, respectively. The case “noARI” turns off aerosol-radiation feedback by setting aerosol optical depth as zero in radiation and photolysis modules. Therefore, the difference between noARI and three other experiments indicates the effect of aerosols in the corresponding mixing state.

3 Results

3.1 Model evaluations

Figure 2 shows the model performance of meteorological parameters (temperature, wind speed and wind direction) in the base experiment (internal mixing). Seen from the profiles, temperature shows a similar pattern between simulation and observation, with the mean bias of 0.7 K and the maximum bias of 1.7 K. The simulated wind direction and wind speed agree well with observation, except that wind speed is overestimated for 1.2~1.9 m/s at 14:00. Comparing the observed and simulated time series at near surface, temperature variation is successfully reproduced, with the maximum bias of about 1.5 K. Wind speed is overestimated for about 2m/s at 16:00 and 17:00. The base experiment reasonably simulates meteorological parameters, which provides the basis for the satisfying simulation of air pollutants.

https://doi.org/10.5194/acp-2022-752
Preprint. Discussion started: 14 November 2022


Atmospheric Chemistry and Physics Discussions

Figure 3 shows the model performance of ozone, $PM_{2.5}$ and BC profiles. The ozone profile shows acceptable performance, with the concentration being underestimated for about 2~12 ppb at 14:00 and 16:00. The simulated $PM_{2.5}$ profile is generally consistent with observations. There is a moderate underestimation of 40~60 μg/m^3 at 11:00 below 800 m and a slight overestimation of about 10~20 μg/m^3 at 14:00. BC profile is almost close to observation, with the maximum bias of about 2~3 μg/m^3. Overall, the model (base experiment) reasonably captures the vertical structure and temporal variation of meteorological elements, $PM_{2.5}$, BC and ozone, which is crucial for exploring the mechanism of aerosol-BL and aerosol-photolysis interactions and explaining their impacts on ozone vertical profile.

3.2 Impact of aerosol-BL interactions

Figure 4a shows the effect of aerosols on PBLH. Aerosols consistently decrease PBLH in all mixing states, with the reduction of 178m (18.5%), 201m (20.9%) and 156m (16.3%) in internal, core-shell and external mixing conditions, respectively. External mixing exerts the weakest PBLH reduction effect here, which is also reported by Gao et al. (2021b). The mechanism of BL suppression by aerosols has been elucidated by many studies (e.g., Ding et al., 2016; Li et al., 2017). The suppression of BL can inhibit turbulent exchange (Figure 4b) and favour the accumulation of precursor contents near the surface. NO_x generally increases at all heights within BL (Figure 4c), and this increase is significantly larger at lower heights than at upper heights. At near surface, the increase is about 4 ppb for internal and core-shell mixing and about 2 ppb for external mixing.

The change in NO_x may alter the ozone chemical regime and influence the sensitivity of ozone to VOC and NO_x. In this study, ozone chemical regime is indicated by $R=H_2O_2/HNO_3$. For Yangtze-River-Delta Region, ozone chemistry is in NO_x-limited regime if $R>0.8$ or in VOC-limited regime if $R<0.6$ or in transition regime if $0.6<R<0.8$ (Qu et al., 2021). The differences in R are small among various aerosol mixing states (Figure 5). Below the height of about 300m, ozone is NO_x-limited during 08:00~10:00 and VOC-limited after 10:00. While at the heights above 300m, ozone is dominantly VOC-limited in the whole daytime. It indicates that despite the change in precursor concentrations, ozone chemical regime almost remains unchanged and it is mainly controlled by VOC. Therefore, the increase in NO_x can enhance NO titration effect and inhibit ozone production, which will be further discussed in Section 3.4. Statistics on the entire model region also show that ozone chemical regime remains unchanged in most areas (>95%) and the dominant type is VOC-limited regime (>92%). Such is the case in the areas with urban or rural surfaces, and in the areas with high or low NO_x emission rates.

3.3 Impact of aerosol-photolysis interactions

The photolysis of NO_2 (JNO_2) and ozone (JO1D) are two major reactions that contribute to ozone production. In noARI condition, photolysis rates increase with height due to atmospheric extinction (figure not shown). When aerosol effect is includ-

https://doi.org/10.5194/acp-2022-752
Preprint. Discussion started: 14 November 2022


Atmospheric Chemistry and Physics Discussions

ed, photolysis rates decrease sharply at lower level but increase at upper level in all mixing states (Figure 6a and b). At the surface level, the relative change of JNO_2 and JO1D in the base experiment (internal mixing) is approximately -30%, which is similar to the value of -22.6% reported by Wu et al. (2020) and -23.0% by Zhao et al. (2021) that conducted in autumn and winter seasons. Notably, in external mixing state, the lower-level decrease is the smallest and the upper-level increase is the largest, with the maximum increase exceeding 10%. Also, the height where photolysis rate (e.g., JNO_2) starts to increase is lower in external mixing state (~500m) than in other mixing states (~1000m).

The significant differences in photolysis change can be explained by aerosol optical properties and its impact on radiation transfer. The aerosol extinction coefficient shows no obvious differences under the three mixing states, with the maximum difference of about 0.05 km^{-1} (Figure 6c). However, the single scatter albedo (SSA) shows distinct differences (Figure 6d). SSA is about 0.8~0.9 in internal and core-shell mixing conditions below 2000m, and it is about 0.90~0.98 in external mixing condition which indicates a strong scattering ability. Zeng et al. (2019) also found that SSA is the largest in external mixing state compared with other mixing states. Therefore, it will backscatter more solar radiation to the upper level (Figure 6e) and promotes photolysis there (Figure 6a and b). Shi et al. (2022) have provided the observational evidence that aerosols can increase shortwave radiation and promote photolysis at the upper level.

3.4 Impact of aerosol-BL and aerosol-photolysis interactions

Figure 7 shows the ozone profile in various mixing states. During 08:00~11:00, the BL is in increasing stage, and ozone increases with height within BL. The average changes in ozone under internal, core-shell and external mixing are -10.3 ppb (-17.1%), -8.7 ppb (-14.5%) and - 3.7 ppb (-6.1%), respectively. As BL develops during 11:00~17:00, ozone shows strong a positive gradient near the surface, uniform distribution above the surface and negative gradient at upper BL. The average change in ozone under internal, core-shell and external mixing is -6.2 ppb (-8.1%), -4.4 ppb (-5.9%) and +0.5 ppb (+0.7%), respectively. During the daytime (08:00~17:00), ozone reduction is larger in internal (9.8%) and core-shell mixing states (7.4%) and the smallest in external mixing state (0.6%). Other studies also reveal that ozone reductions caused by aerosols are approximately in the range of 10~20% (e.g., Gao et al., 2020; Qu et al., 2021; Yang et al., 2022). It can be inferred that ozone concentration is generally reduced in all mixing states and at all heights within BL. The reduction is the smallest in external mixing state, and the ozone below about 1000m shows a slight increase after 11:00 (Figure 7b). It could be because the enhanced NO titration effect associated with NO_x accumulation is weaker in external mixing than in other mixing states (Figure 4c). Also, externally mixed aerosols lead to less photolysis suppression in the lower level and larger photolysis enhancement in the upper level (Figure 6a and b), which will partly counteract the reduction in ozone concentration.

To illustrate the mechanism of aerosols affecting ozone variation, we perform process analysis on ozone (Zhang et al., 2014).

https://doi.org/10.5194/acp-2022-752
Preprint. Discussion started: 14 November 2022


Atmospheric Chemistry and Physics Discussions

In this study, ozone is decomposed into vertical mixing (VMIX), net chemical production (CHEM) and advection (ADVC; including horizontal and vertical advection) (Figure 8). The sign of CHEM depends on the competition between ozone production and loss. Under the effect of aerosols, CHEM shows negative change at near surface and positive change from lower to upper BL (Figure 8f-h). The negative CHEM change can be explained by the decrease in photolysis rate (Figure 6a and b) and the increase in NO titration associated with NO_x accumulation (Figure 4c). Photolysis reduction may inhibit ozone production, and the increased NO titration consumes more ozone under VOC-limited regime (Figure 5f). From lower to upper BL, the positive CHEM change is dominantly contributed by the significant photolysis enhancement (Figure 6a and b). Since photolysis enhancement is the strongest in external mixing state, the increase in CHEM at 300~800m is the largest compared with other mixing states (Table 3). Above BL, especially between the solid and dash lines, the change in CHEM is negative due to the inhibited turbulent transport of NO_x from the BL.

The variation in ozone photochemistry indicated by CHEM can influence VMIX which depends on ozone vertical gradient and turbulent exchange. In noARI condition, VMIX presents three distinct entrainment zones according to its signs: positive zone near the surface, negative zone at lower-to-middle BL, and time-variant zone at upper BL (near PBLH). VMIX is positive near the surface and negative at lower-to-middle BL (Figure 8a), because the higher concentration of ozone aloft is entrained downward by turbulent mixing. The time-variant VMIX zone at upper BL, specifically, negative values during 08:00~11:00 and positive values during 11:00~16:00 (Figure 8a), is determined by the relationship between PBLH diurnal variation and ozone vertical gradient below PBLH. During 08:00~11:00, ozone gradient at upper BL is positive (Figure 7a), which causes entrainment loss at that height. Above BL where ozone gradient and turbulent mixing are weak, ozone vertical exchange is not significant. Consequently, VMIX is negative at upper BL. During 11:00~16:00, ozone gradient at upper BL is negative (Figure 7b), which causes entrainment gain at that height and the positive VMIX at upper BL. Under the effect of aerosols, VMIX notably increases near the surface and decreases above surface in all mixing states especially after 11:00 (Figure 8b-d). It is because that the reinforced NO titration effect near surface and the enhanced photolysis aloft strengthen the ozone vertical gradient. The increase in gradient promotes ozone vertical exchange, compensating for the weakened ozone entrainment due to turbulent suppression, and instead, more ozone aloft are entrained to near surface (Gao et al., 2020, 2021a). At upper BL, the change in VMIX is negative during 08:00~11:00 and positive during 11:00~16:00. It is possibly due to that the negative and positive VMIX zones in Figure 8a move downward as PBLH decreases. The change in ADVC is generally positive (Figure 8j-l), and its contribution is relatively not important compared with VMIX and CHEM.

Table 3 quantitatively describes the respective contributions of three processes to ozone variation during 11:00~17:00. From near surface to lower BL (0~300m), the positive VMIX contribution is stronger than the negative CHEM contribution, and the role of ADVC can be ignored. At lower-to-middle BL (300~800m), the promoting effect of VMIX on ozone weakens, and instead, the negative contribution of CHEM turns to positive and becomes the dominant influencing factor. At the upper

https://doi.org/10.5194/acp-2022-752
Preprint. Discussion started: 14 November 2022


Atmospheric Chemistry and Physics Discussions

206 BL (800~1500m), VMIX plays the dominant role due to the increasing ozone entrainment at upper BL (Figure 8b-d). The
207 relative contributions of the three processes are generally consistent in all mixing states.

208 4 Discussions

209 Above we have presented the variation in photolysis rates, ozone precursors and ozone concentration induced by aerosols. To
210 make the results more convincing, we perform additional analysis and simulations. The effect of aerosols on ozone may de-
211 pend on the underlying surface type, e.g., urban and rural surfaces (Zhu et al., 2015). From Table 4, differences between ur-
212 ban and rural are not obvious. Ozone shows a consistent decreasing and NO_x shows a consistent increasing feature under the
213 effect of aerosols. Photolysis rate (e.g., JNO_2) presents the dual change (i.e., lower-level decreasing and upper-level increas-
214 ing). Comparing the three mixing types, the changes in photolysis rates, ozone precursors and ozone concentration caused by
215 externally mixed aerosols are most favourable for mitigating ozone reduction. The mechanisms have been explained in pre-
216 vious sections.

217 We extend the simulations for 3 days (2 November 20:00 to 5 November 20:00) to examine the aerosol effect under different
218 pollution conditions (Figure 9). The extended periods are relatively clean conditions, with the average $PM_{2.5}$ being about 1/3
219 of 2 November. In this clean episode, the NO_x variation also shows the same pattern as Figure 4. Photolysis rate still exhibits
220 dual changes in external mixing state, while it decreases at all heights in internal and core-shell mixing states. Ozone con-
221 centration is also reduced and the reduction is the smallest in external mixing condition. Due to the relatively low aerosol
222 content during this period, the changes in these quantities are much weaker than those during the pollution episode (2 No-
223 vember). It can be inferred that aerosol effect on photolysis rates, ozone precursors and ozone concentration might be con-
224 sistent under different underlying surface and pollution conditions, and it is more significant in polluted conditions.

225 5 Conclusions

226 Previous studies mainly focus on the relationship between aerosols and ozone at near surface and attribute ozone variation to
227 either aerosol-BL or aerosol-photolysis interactions. In this work, we explore the sensitivities of ozone response to aerosol
228 mixing states in the vertical direction by WRF-Chem simulations during an air pollution case from 2 to 5 November 2020 in
229 Nanjing. Generally, the model reasonably captures the vertical profiles and temporal variation of meteorological elements,
230 ozone, $PM_{2.5}$ and BC. Sensitive experiments show that:

231 Aerosols influence ozone vertical variation through aerosol-BL and aerosol-photolysis interactions. Aerosol inhibits BL de-

https://doi.org/10.5194/acp-2022-752
Preprint. Discussion started: 14 November 2022


Atmospheric Chemistry and Physics Discussions

velopment, resulting in more NO_x accumulated within BL and a stronger NO titration effect under VOC limited regime. The PBLH reduction and NO_x accumulation are the smallest in external mixing state. Despite the change in precursor concentration, ozone chemical regime is still dominantly controlled by VOC (>95%) under different underlying surface and emission conditions. Aerosols inhibit photolysis at lower level (~-30%) but enhance photolysis at upper level (~10%) due to aerosol backscattering. The enhanced photolysis is more obvious in external mixing state owing to its strong scattering ability.

Aerosols basically lead to ozone reduction (0~10%) at all heights within BL during the daytime (08:00~17:00), with the least reduction (0.5%) and a slight increase (0.7%) in external mixing state after 11:00. Such ozone variation is attributed to the changes in VMIX, CHEM and ADVC. CHEM decreases at near surface due to photolysis reduction and NO_x accumulation, but increases from lower to upper BL due to photolysis enhancement. The photolysis reduction and NO_x accumulation at lower level lead to ozone depletion and stronger vertical gradient, which promotes higher concentration of ozone aloft being entrained downward. Therefore, VMIX increases at near surface but decreases at lower-to-middle BL. VMIX variation at upper BL (near PBLH) is complex, which is determined by the relationship between PBLH diurnal variation and ozone gradient near PBLH. Quantitative comparisons among these processes show that: From near surface to lower BL (0~300m), positive VMIX contribution outweighs the negative CHEM contributions. At lower-to-middle BL (300~800m), positive VMIX contribution decreases, and CHEM becomes the dominant positive contributor. At upper BL (800~1500m), VMIX plays the dominant role. Additional analysis and simulations indicate that aerosols could consistently cause precursor accumulation, dual change of photolysis and ozone reduction under different underlying surface and pollution conditions.

Code and data availability. Some of the data repositories have been listed in Section 2. The other data, model outputs and codes can be accessed by contacting Bin Zhu via binzhu@nuist.edu.cn.

Author contributions. SY performed the model simulation, data analysis and manuscript writing. BZ proposed the idea, supervised this work and revised the manuscript. SS provided the data at observation site. WL, JG and HK offered helps to the model simulation. DL helped the revision of the manuscript.

Competing interests. The authors declare that they have no conflict of interest.

Acknowledgements. This work is supported by the National Natural Science Foundation of China (Grant Nos. 92044302, 42192512 and 42275115).

https://doi.org/10.5194/acp-2022-752
Preprint. Discussion started: 14 November 2022

Atmospheric Chemistry and Physics Discussions

References

Bond, T. C., Habib, G., and Bergstrom, R. W.: Limitations in the enhancement of visible light absorption due to mixing state, J. Geophys. Res., 111, 360, https://doi.org/10.1029/2006JD007315, 2006.

Dickerson, R. R., Kondragunta, S., Stenchikov, G., Civerolo, K. L., Doddridge, B. G., and Holben, B. N.: The impact of aerosols on solar ultraviolet radiation and photochemical smog, Science, 278, 827–830, https://doi.org/10.1126/science.278.5339.827, 1997.

Ding, A. J., Huang, X., Nie, W., Sun, J. N., Kerminen, V. M., Petaja,T., Su, H., Cheng, Y. F., Yang, X. Q., Wang, M. H., Chi, X. G.,Wang, J. P., Virkkula, A., Guo, W. D., Yuan, J., Wang, S. Y., Zhang, R. J., Wu, Y. F., Song, Y., Zhu, T., Zilitinkevich, S., Kulmala, M., and Fu, C. B.: Enhanced haze pollution by black carbon in megacities in China, Geophys. Res. Lett., 43, 2873–2879, https://doi.org/10.1002/2016GL067745, 2016.

Fu, Y., Liao, H., & Yang, Y.: Interannual and decadal changes in tropospheric ozone in China and the associated chemistry–climate interactions: A review, Adv. Atmos. Sci., 36(9), 975–993, https://doi.org/10.1007/s00376-019-8216-9, 2019.

Gao, J., Zhu, B., Xiao, H., Kang, H., and Pan, C.: Effects of black carbon and boundary layer interaction on surface ozone in Nanjing, China, Atmos. Chem. Phys., 18, 7081-7094, https://doi.org/10.5194/acp-2017-1177, 2018.

Gao, J., Li, Y., Zhu, B., Hu, B., Wang, L., and Bao, F.: What have we missed when studying the impact of aerosols on surface ozone via changing photolysis rates?, Atmos. Chem. Phys., 20, 10831–10844, https://doi.org/10.5194/acp-20-10831-2020, 2020.

Gao, J., Li, Y., Xie, Z., Wang, L., Hu, B., and Bao, F.: Do Absorbing Aerosols or Scattering Aerosols Dominate the Impact of Aerosols on Ozone via Influencing Photolysis Rates?, Earth and Space Science Open Archive, https://doi.org/10.1002/essoar.10508565.1, 2021a.

Gao, M., Yang, Y., Liao, H., Zhu, B., Zhang, Y., Liu, Z., Lu, X., Wang, C., Zhou, Q., Wang, Y., Zhang, Q., Carmichael, G. R., and Hu, J.: Reduced light absorption of black carbon (BC) and its influence on BC-boundary-layer interactions during "APEC Blue", Atmos. Chem. Phys., 21, 11405–11421, https://doi.org/10.5194/acp-21-11405-2021, 2021b.

Jacob, D. J.: Heterogeneous chemistry and tropospheric ozone, Atmospheric Environ., 34, 2131-2159, https://doi.org/10.1016/S1352-2310(99)00462-8, 2000.

Jacobson, M. Z. Studying the effects of aerosols on vertical photolysis rate coefficient and temperature profiles over an urban airshed, J. Geophys. Res.: Atmos., 103(D9), 10593, https://doi.org/10.1029/98JD00287, 1998.

Jacobson, M. Z.: Strong radiative heating due to the mixing state of black carbon in atmospheric aerosols, Nature, https://doi.org/10.1038/35055518, 2001.

Li, J., Wang, Z., Wang, X., Yamaji, K., Takigawa, M., Kanaya, Y.: Impacts of aerosols on summertime tropospheric photolysis frequencies and photochemistry over central eastern china, Atmos. Environ., 45(10), 1817-1829, https://doi.org/10.1016/j.atmosenv.2011.01.016, 2011.

Li, K., Jacob, D. J., Liao, H., Zhu, J., Shah, V., Shen, L., Bates, K., Zhang, Q., & Zhai, S.: A two-pollutant strategy for improving ozone and particulate matter air quality in China, Nat. Geosci., 12, 906-910, https://doi.org/10.1038/s41561-019-0464-x, 2019.

Li, K., Jacob, D. J., Shen, L., Lu, X., de Smedt, I., & Liao, H.: Increases in surface ozone pollution in China from 2013 to 2019: anthropogenic and meteorological influences, Atmos. Chem. Phys., 20, 11423-11433, https://doi.org/10.5194/acp-20-11423-2020, 2020.

Li, Y., Cao, L., Gao, S., and Luo, B.: The Current Stage and Development of MICAPS, Meteorological Monthly, 36, 50–55,

2010 (in Chinese).

Li, Z. Q., Guo, J. P., Ding, A. J., Liao, H., Liu, J. J., Sun, Y. L., Wang, T. J., Xue, H. W., Zhang, H. S., and Zhu, B.: Aerosol and boundary-layer interactions and impact on air quality, Natl. Sci. Rev., 4, 810–833, https://doi.org/10.1093/nsr/nwx117, 2017.

Lou, S., Liao, H., & Zhu, B.: Impacts of aerosols on surface-layer ozone concentrations in China through heterogeneous reactions and changes in photolysis rates, Atmos. Environ., 85, 123-138, doi:10.1016/j.atmosenv.2013.12.004, 2014.

Qu, Y., Voulgarakis, A., Wang, T., Kasoar, M., Wells, C., Yuan, C., Varma, S., and Mansfield, L.: A study of the effect of aerosols on surface ozone through meteorology feedbacks over China, Atmos. Chem. Phys., 21, 5705–5718, https://doi.org/10.5194/acp-21-5705-2021, 2021.

Shi, S., Zhu, B., Lu, W., Yan, S., Fang, C., Liu, H., Liu, D., Liu, C.: Estimation of radiative forcing and heating rate based on vertical observation of black carbon in Nanjing, China, Sci. Tot. Environ., https://doi.org/10.1016/j.scitotenv.2020.144135, 2020.

Shi, S., Zhu, B., Tang, G., Liu, C., An, J., Liu, D., Xu, J., Xu, H., Liao, H., & Zhang, Y.: Observational evidence of aerosol radiation modifying photochemical ozone profiles in the lower troposphere, Geophys. Res. Lett., 49, e2022GL099274, https://doi. org/10.1029/2022GL099274, 2022.

Wu, J., Bei, N., Hu, B., Liu, S., Wang, Y., Shen, Z., Li, X., Liu, L., Wang, R., Liu, Z., Cao, J., Tie, X., Molina, L. T., and Li, G.: Aerosol-photolysis interaction reduces particulate matter during wintertime haze events, Proc. Natl. Acad. Sci. USA, 117, 9755–9761, https://doi.org/10.1073/pnas.1916775117, 2020.

Yang, H., Chen, L., Liao, H., Zhu, J., Li, X.: Impacts of aerosol-photolysis interaction and aerosol-radiation feedback on surface-layer ozone in north china during a multi-pollutant air pollution episode, Atmos. Chem. Phys., 22(6), 4101–4116, https://doi.org/10.5194/acp-2021-1192022, 2022.

Zaveri, R. A. and Peters, L. K.: A new lumped structure photochemical mechanism for large-scale applications, J. Geophys. Res., 104, D23, 30387–30415, https://doi.org/10.1029/1999JD900876, 1999.

Zaveri, R. A., Easter, R. C., Fast, J. D., and Peters, L. K.: Model for simulating aerosol interactions and chemistry (MOSAIC), J. Geophys. Res., 113, D13204, https://doi.org/10.1029/2007JD008782, 2008.

Zeng, C., Liu, C., Li, J., Zhu, B., Yin, Y., and Wang, Y.: Optical Properties and Radiative Forcing of Aged BC due to Hygroscopic Growth: Effects of the Aggregate Structure, J. Geophys. Res. Atmos., 124, 4620–4633, https://doi.org/10.1029/2018JD029809, 2019.

Zhang, H., DeNero, S. P., Joe, D. K., Lee, H.-H., Chen, S.-H., Michalakes, J., and Kleeman, M. J.: Development of a source oriented version of the WRF/Chem model and its application to the California regional PM10/PM2.5 air quality study, Atmos. Chem. Phys., 14, 485–503, https://doi.org/10.5194/acp-14-485-2014, 2014.

Zhao, S., Hu, B., Liu, H., Du, C., Xia, X., & Wang, Y.: The influence of aerosols on the NO2 photolysis rate in a suburban site in North China, Sci. Total Environ., 767, 144788, https://doi.org/10.1016/j.scitotenv.2020.144788, 2021.

Zheng, B., Tong, D., Li, M., Liu, F., Hong, C., Geng, G., Li, H., Li, X., and Peng, L.: Trends in China's anthropogenic emissions since 2010 as the consequence of clean air actions, Atmos. Chem. Phys., 18, 14095–14111, https://doi.org/10.5194/acp-18-14095-2018, 2018.

Zhu, B., Kang, H. Q., Zhu, T., Su, J. F., Hou, X. W., and Gao, J. H.: Impact of Shanghai urban land surface forcing on downstream city ozone chemistry, J. Geophys. Res.-Atmos., 120, 4340–4351, https://doi.org/10.1002/2014JD022859, 2015.

https://doi.org/10.5194/acp-2022-752
Preprint. Discussion started: 14 November 2022

Atmospheric Chemistry and Physics Discussions

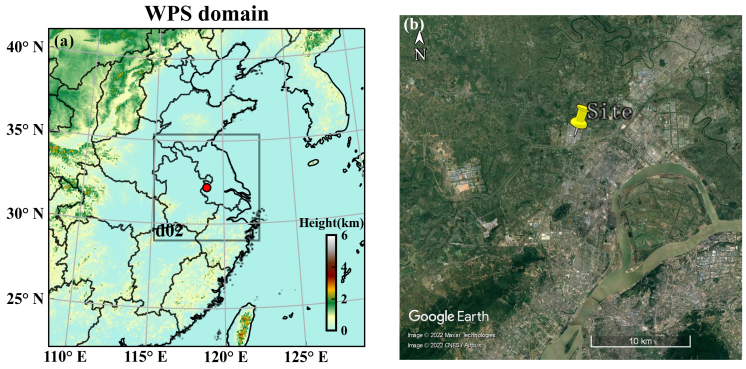

337

338 Figure 1. The model simulation domain (a) and the surrounding area of the observation site (b). The red point in (a)
339 and the yellow symbol in (b) are the observation site.
340

https://doi.org/10.5194/acp-2022-752
Preprint. Discussion started: 14 November 2022

Atmospheric Chemistry and Physics Discussions

341

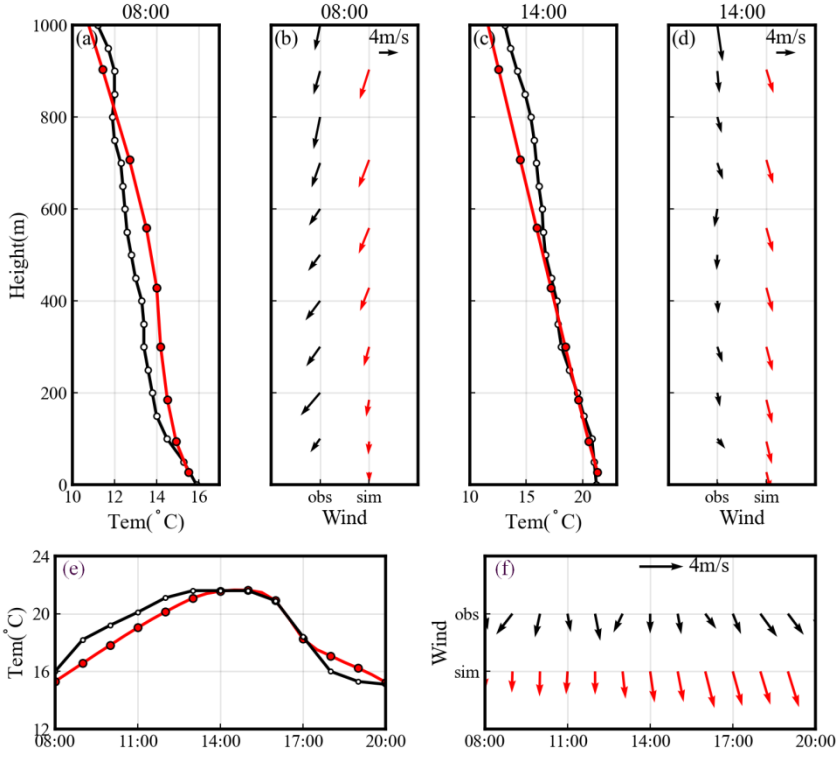

342

343 Figure 2. Model evaluations of temperature and wind. The first row is the profile and the second row is the time se-
344 ries at near surface. The black color is observation and red color is simulation.
345

https://doi.org/10.5194/acp-2022-752
Preprint. Discussion started: 14 November 2022

Atmospheric Chemistry and Physics Discussions

346

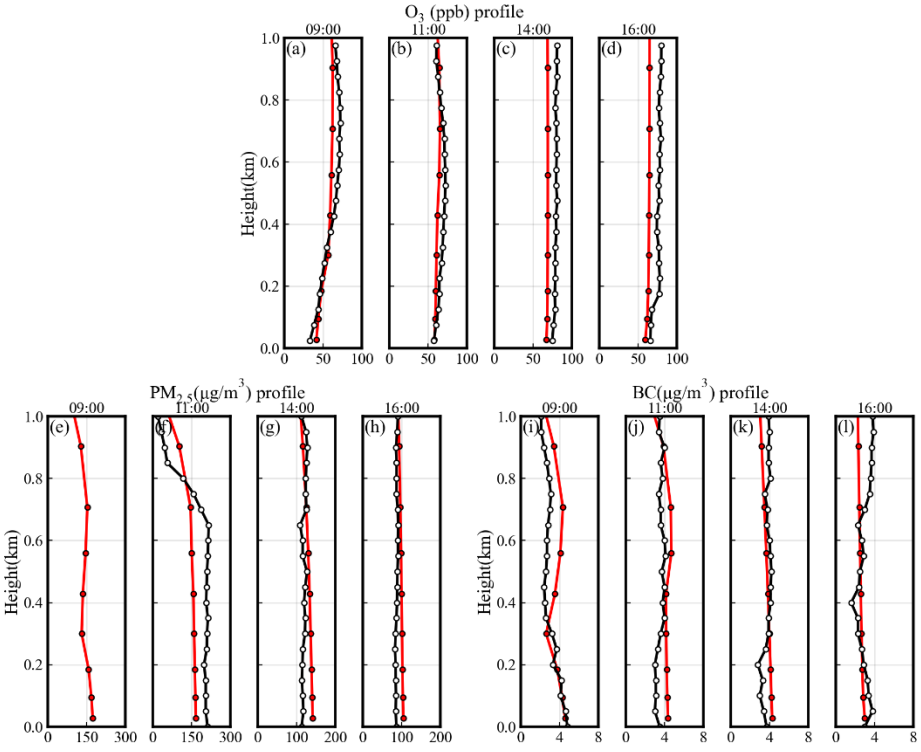

347

348 Figure 3. Model evaluations of ozone, $PM_{2.5}$ and BC profiles. The black color is observation and red color is simula-
349 tion. The $PM_{2.5}$ observation data at 09:00 is missing due to instrument failure.
350

https://doi.org/10.5194/acp-2022-752
Preprint. Discussion started: 14 November 2022

Atmospheric Chemistry and Physics Discussions

351

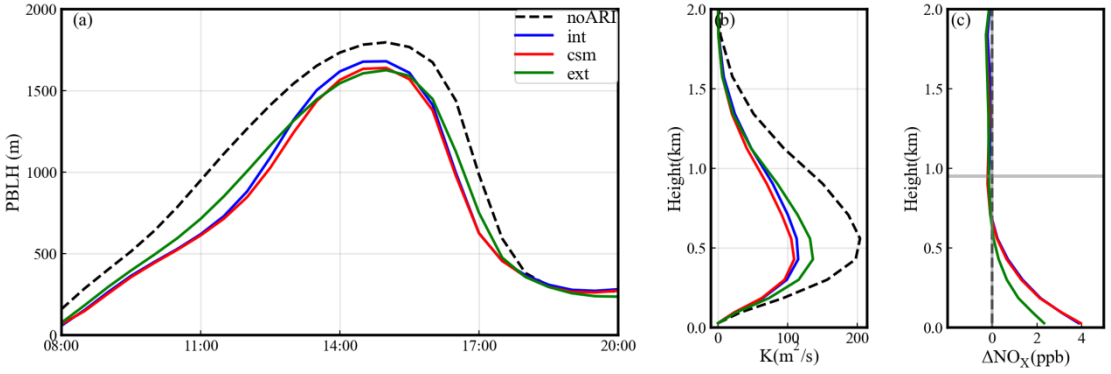

352

353 Figure 4. Time series of PBLH (a), profile of turbulent exchange coefficient K (b) and aerosol-induced change of
354 NO_x profile (c) under different mixing states. The horizontal line in (c) is the PBLH of the base experiment. The pro-
355 files and PBLH in (c) are averaged during 08:00~17:00.

356

https://doi.org/10.5194/acp-2022-752
Preprint. Discussion started: 14 November 2022

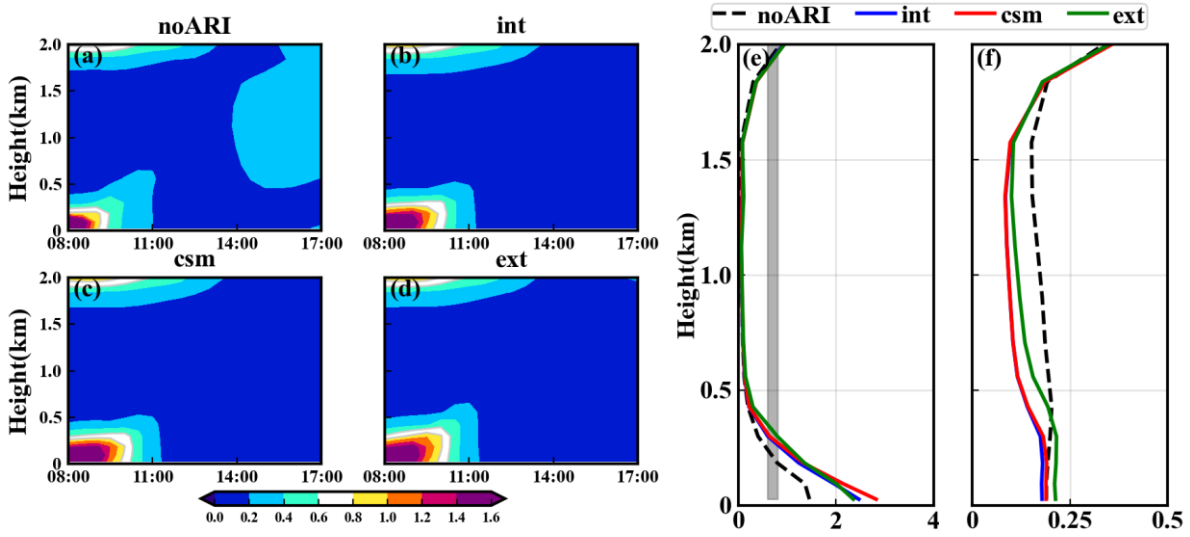

Figure 5. (a-d) Time-height distribution of ozone chemical regime (indicated by $R=H_2O_2/HNO_3$) in different aerosol mixing states. (e-f) Profiles of R averaged during 08:00~10:00 and 10:00~17:00, respectively. The white contours in (a-d) and the grey strips in (e-f) represent the transition regime (0.6<R<0.8).

https://doi.org/10.5194/acp-2022-752
Preprint. Discussion started: 14 November 2022

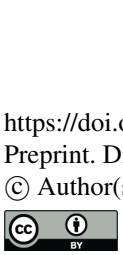

Atmospheric Chemistry and Physics Discussions

362

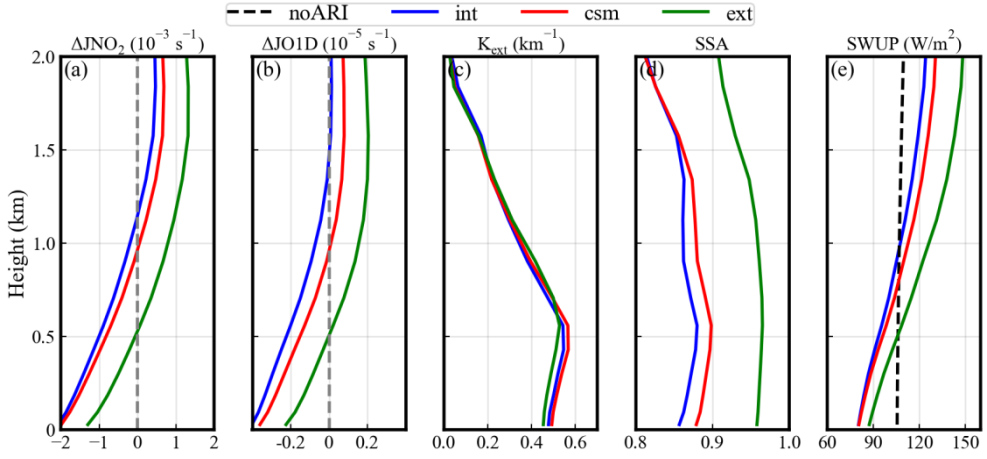

363

364 Figure 6. Comparisons of JNO_2 (a), JO1D (b), aerosol extinction coefficient (c), single scatter albedo (d) and
365 upwelling shortwave flux (e) profiles among different mixing states. For JNO_2 and JO1D, the profiles are the changes
366 with respect to noARI condidition. Profiles are time averages during 11:00~17:00.
367

https://doi.org/10.5194/acp-2022-752
Preprint. Discussion started: 14 November 2022

Atmospheric Chemistry and Physics Discussions

368

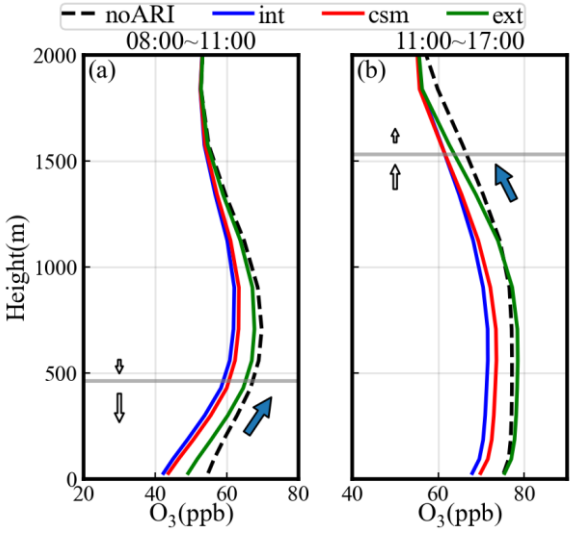

369

370 Figure 7. Ozone profiles under different mixing states. (a) 08:00~11:00 average. (b) 11:00~17:00 average. The hori-
371 zontal line is PBLH. The blue arrows highlight the ozone vertical gradient at corresponding heights. The white arrows
372 qualitatively describe the direction and magnitude of ozone turbulent exchange at the corresponding heights above or
373 below PBLH.

374

https://doi.org/10.5194/acp-2022-752
Preprint. Discussion started: 14 November 2022

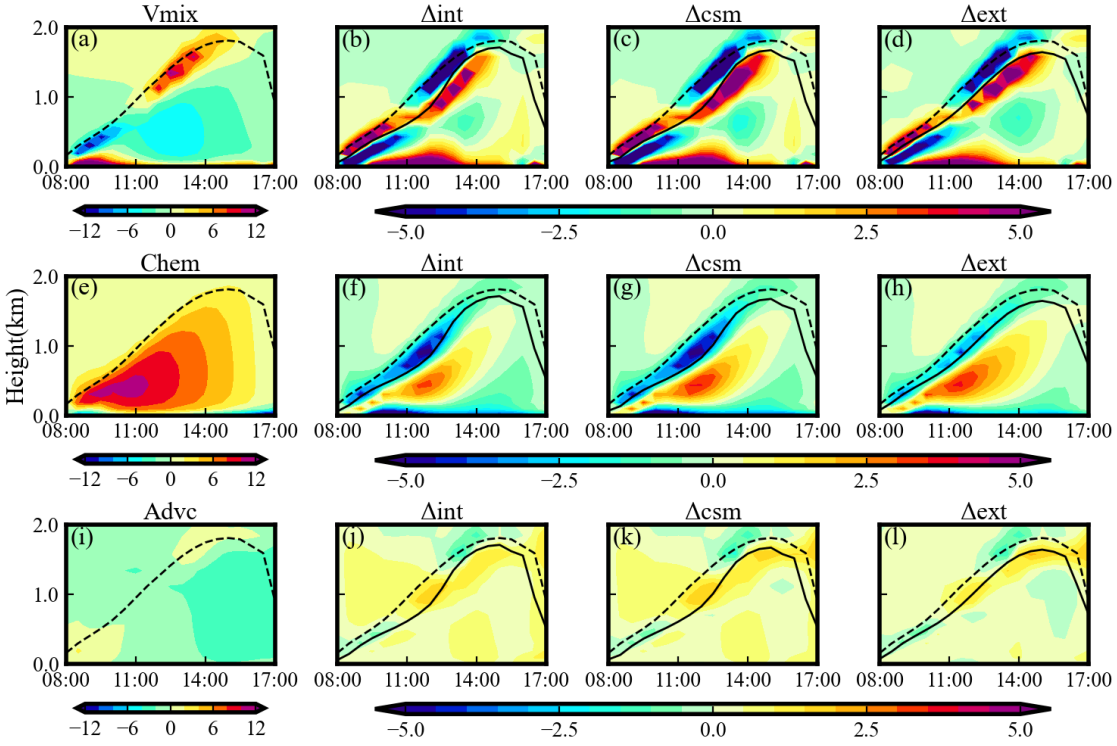

Figure 8. The time-height distribution of process tendencies (ppb/h) that contribute to ozone variation. The three rows are Vmix, Chem and Advc, respectively. The first column is the ozone tendency in noARI condition, and the rest three columns are the changes in ozone tendency under different aerosol mixing states.

https://doi.org/10.5194/acp-2022-752
Preprint. Discussion started: 14 November 2022

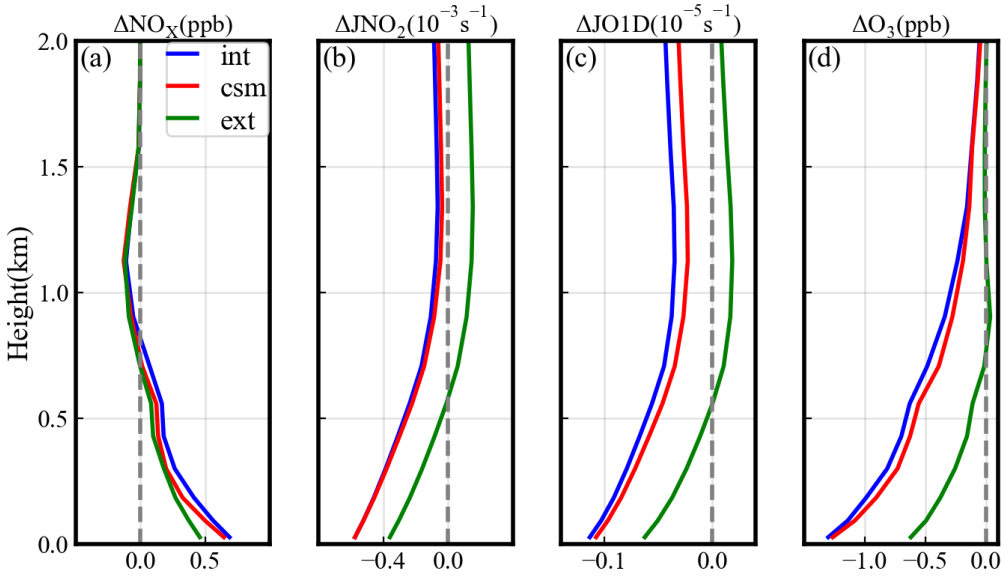

Figure 9. The diurnal averaged profile (08:00~17:00) of the changes in NO_x, JNO_2, JO1D and ozone caused by aerosols during the clean episode (the extended simulation during 3~5 November).

https://doi.org/10.5194/acp-2022-752
Preprint. Discussion started: 14 November 2022


Atmospheric Chemistry and Physics Discussions

384 Table 1. Physical and chemical parameterization schemes.

Scheme	Option
Boundary layer	YSU
Microphysics	Lin
Longwave radiation	RRTMG
Shortwave radiation	RRTMG
Land surface	Noah
Grid nudging	On
Observation nudging	Off
Gas phase chemistry	CBMZ
Aerosol chemistry	MOSAIC-4bin
Aerosol-radiation feedback	On
Aerosol optical properties	Varies with experiments

385

https://doi.org/10.5194/acp-2022-752
Preprint. Discussion started: 14 November 2022


Atmospheric Chemistry and Physics Discussions

386 Table 2. Settings of sensitive experiments.

Case name	Aerosol mixing states
int	internally mixed; base experiment
csm	core-shell mixed
ext	externally mixed
noARI	turn off aerosol-radiation feedback
Effect	**Description**
Δint=int-noARI	effect by internal mixing
Δcsm=csm-noARI	effect by core-shell mixing
Δext=ext-noARI	effect by external mixing

387
388

https://doi.org/10.5194/acp-2022-752
Preprint. Discussion started: 14 November 2022

Atmospheric Chemistry and Physics Discussions

389 Table 3. The contribution of aerosol to ozone process tendencies (ppb/h) under different mixing states during
390 11:00~17:00. The values are averaged below the PBLH. The parentheses are relative contributions of each process, e.g.,
391 Δvmix/(|Δvmix| + |Δchem| + |Δadvc|)*100%.

	int	csm	ext
H: 0~300m			
Δvmix	+2.9 (+53.2%)	+2.8 (+53.7%)	+2.3 (+57.4%)
Δchem	-2.2 (-39.5%)	-2.0 (-38.7%)	-1.5 (-37.3%)
Δadvc	+0.4 (+7.4%)	+0.4 (+7.5%)	+0.2 (+5.4%)
H: 300~800m			
Δvmix	+0.0 (+3.0%)	-0.2 (+13.2%)	-0.4 (-25.1%)
Δchem	+0.5 (+52.6%)	+0.5 (+57.6%)	+0.8 (+65.8%)
Δadvc	+0.4 (+44.4%)	+0.4 (+29.1%)	+0.2 (+9.2%)
H: 800~1500m			
Δvmix	-1.5 (+71.9%)	+2.0 (+79.0%)	+1.4 (+65.5%)
Δchem	+0.1 (+3.1%)	-0.0 (-0.3%)	+0.6 (+28.2%)
Δadvc	+0.5 (+25.1%)	+0.5 (+20.7%)	+0.1 (+6.3%)

392

https://doi.org/10.5194/acp-2022-752
Preprint. Discussion started: 14 November 2022


Atmospheric Chemistry and Physics Discussions

393 Table 4. The diurnal averaged (08:00~17:00) variations of ozone, NO_x and JNO_2 variations caused by different aero-
394 sol mixing states in urban and rural conditions. The statistics are conducted at the entire model grids.

	Δint	Δcsm	Δext
ΔOzone (ppb) (0.0~1.5km)			
urban	-6.4(-9.4%)	-4.9(-7.2%)	-0.4(-0.6%)
rural	-6.7(-10.1%)	-5.1(-7.8%)	-0.4(-0.6%)
ΔNO_x (ppb) (0.0~1.5km)			
urban	+0.8(+17.2%)	+0.8(+15.3%)	+0.3(+6.8%)
rural	+0.6(+20.4%)	+0.5(+17.7%)	+0.2(+6.2%)
ΔJNO_2 ($10^{-3}s^{-1}$) (0.0~1.0km)			
urban	-0.9(-16.8%)	-0.8(-14.5%)	-0.2(-3.9%)
rural	-1.0(-17.1%)	-0.9(-14.7%)	-0.2(-3.7%)
ΔJNO_2 ($10^{-3}s^{-1}$) (1.0~1.5km)			
urban	+0.1(+2.0%)	+0.3(+4.9%)	+1.0(+14.3%)
rural	+0.1(+1.2%)	+0.3(+4.4%)	+1.1(+14.9%)

395